The thermal conductivity of polyamorphous state of solid monohydroxyl alcohols

A.I. Krivchikov, O.A. Korolyuk, and I.V. Sharapova

B. Verkin Institute for Low Temperature Physics and Engineering of the National Academy of Sciences of Ukraine
47 Lenin Ave., Kharkov 61103, Ukraine
E-mail: krivchikov@ilt.kharkov.ua

New measurement results on the thermal conductivity of solid ethyl alcohol C_2H_5OH in the interval from 2 K to the melting temperature are presented. The annealing effect in the thermal conductivity of the orientationally ordered phase of the alcohol has been observed in a wide range of temperatures. This phase was obtained as a result of the irreversible first-order phase transition from an orientationally disordered crystal of cubic structure at $T = 109$ K. The thermal conductivity was observed to increase as the monoclinic lattice changed from a less stable phase to a more stable one. The growth may be due to the improved quality of the completely ordered crystal. A comparative analysis of the temperature dependences of thermal conductivity $\kappa(T)$ was performed for solid monohydroxyl alcohols CH_3OH, C_2H_5OH, C_2D_5OD, C_3H_7OH and C_4H_9OH in the disordered orientational and structural states. At low temperatures the thermal conductivity of a series of monohydroxyl structural glasses of alcohols increases with the mass of the alcohol molecule by a linear dependence.

1. Introduction

At present a molecular glasses have been attracting a special interest in solid state physics because some of them enable recognizing the importance of orientational degrees of freedom in the dynamics of glasses [1–7]. There is no long-range order of molecules in molecular glass. At low temperatures the properties of structural glasses are essentially different from those of the corresponding completely ordered equilibrium crystals. For example, the heat capacity is always higher and the thermal conductivity is always lower in glasses than in corresponding crystals. The thermal conductivity $\kappa(T)$ of a glass is weakly dependent on the structure or the chemical composition of a substance [8]. The temperature dependence of the thermal conductivity of a glass has three distinct regions: a low-temperature region in which $\kappa(T)$ grows with temperature as $\kappa(T) \sim T^2$, a plateau in the interval $T = 5$–30 K and a region above T_{plateau} in which $\kappa(T)$ continues to increase by a quasilinear law.

Several phenomenological models and theories have been developed to explain the detected features of the thermal properties of glasses, which in addition to sound waves, involve low-energy elementary excitations: two-level tunneling systems (TLS) [9,10] and relaxation systems [11] and low-frequency quasilocal vibrational modes. The soft-potential model (SPM) is based on a single approach to two-level systems, relaxation systems and low-frequency vibrational modes and can be considered as a generalization of the models of two-level systems and low-frequency vibraitonal modes [12,13]. Two parameters were introduced to describe elementary excitations in a wide interval of energies: the characteristic energy W assigns the energy scale of the classification of elementary excitations in the harmonic soft potential and the parameter C relates the phonon and two-level systems. At present the SPM has been used widely to describe the thermal properties of glasses.

According to resent data [7], ethanol glass is a special case in the mentioned series of glasses. It belongs to type II glasses [7] which form an orientationally disordered plastic phase. Pure ethanol is without doubt the most interesting object among molecular substances for investigations of thermal properties of one-component molecular solids with disordering. Solid ethanol at some conditions can have three metastable long-lived states with molecular disorder in addition to the thermodynamically stable fully orienta-

tionally ordered crystalline phase (FOC, monoclinic, $Z = 4$, Pc): a structural glass (SG), an orientational glass (OG, bcc) and a plastic crystal of a cubic structure with orientational dynamic disorder (RPC) (e.g., see [1,3,5,14]). On fast cooling the liquid ethanol becomes supercooled and transforms into a structural glass below the glass transition temperature T_g. Orientational glass (OG, an orientationally disordered crystal) is another type of molecular disorder in molecular glasses — an orientational disorder which coexists with a translational order. The temperature dependences of the Gibbs energy in the state diagram [1,3,5,14] was shown that the OG phase of ethanol is formed by cooling a metastable state of plastic crystal (i.e., crystal with rotational disorder). In ethanol the temperature of freezing is about the glass transition temperature T_g of supercooled liquid (SCL). Since these temperature regions coincide for the SG and OG states of ethanol, it is easy to compare the temperature dependences of the thermal conductivity of these states within one temperature interval and see how the orientational degrees of freedom of molecules influence the heat transfer in a glass-state alcohol. The investigations by the methods of calorimetry, Brillouin light scattering and x-ray diffraction have shown [15] that the phase diagram of solid ethyl alcohol under equilibrium vapor pressure is more complex than it was thought before. At least four types of different monoclinic structures (which calls as α, β, γ, and δ structure), which appears at different prepare conditions, can be separated in the orientationally ordered phase having a monoclinic lattice with orientational long-range order. The metastable monoclinic state (α structure) is formed at solid-state transformations of cubic structure (RPC) to monoclinic structure.

Alcohols are the simplest molecular systems with hydrogen bond to study physical phenomena in glass at low temperatures. Primary monohydroxyl (normal) alcohols have a single OH group fixed to the carbon skeleton. The general formula of an alcohol is $H(CH_2)_nOH$, where n is the number of C atoms in an alcohol molecule. In the primary alcohol series from methanol to 1-butanol the mass of an alcohol molecule grows and the effect of the cooperative hydrogen bond weakens as the number of C atoms in the molecule increases. These factors influence the interaction energy of alcohol molecules and the properties (glass formation, thermal, etc.) of glasses. For example, methanol has the poorest glass-forming property in this series of alcohols. Glass can form in it only on adding a small quality of water [16].

In this study a new results on the thermal conductivity of solid protonated ethyl alcohol are presented. The effect of annealing in the thermal conductivity (relaxation of the thermal conductivity) of solid ethanol in the orientationally ordered phase has been observed. This phase was obtained as a result of a solid-state transition from an orientationally disordered crystal of cubic structure. It is shown that annealing causes structural changes in an OG sample of pro-

tonated ethanol as it approaches its thermodynamic equilibrium. The changes resemble those observed on annealing 1-butanol (SG → exotic "glacial" state → FOC).

In this work we compare and generalize the previous experimental data on the thermal conductivity of the homological series of monohydroxyl alcohols from methanol to 1-butanol in the state of structural glass, the thermal conductivity of structural and orientational glasses of protonated and deuterated ethanol. It is shown that the new features of the thermal conductivity of the investigated glasses are attributed to the influence of the orientational degrees of freedom of molecules.

2. Experimental results. Discussion

2.1. Material. Preparation of structural glass

According to the chromatographic analysis, the water content in pure methanol was less than 0.2% H_2O. The water–methanol solution contained 6.6 mol. % H_2O [17]. Liquid ethanol C_2H_5OH 96% (SWW 2442-90) produced by Polskie Odczynniki Chemiczne S.A. was purified up to 99.9% (according to chromatogram method) directly before the thermal conductivity measurement. The deuterated C_2D_5OD alcohol (D purity was 99%, anhydrous) was supplied by Cambridge Isotope Laboratories, Inc. [18]. Material of 1-propanol with a stated purity of 99.9% (Chromasolv for high-performance liquid chromatography, SIGMA-ALDRICH Chemie Gmbh) were used [19]. High-purity samples of 1-butanol (Aldrich, anhydrous grade, $\geq 99.8\%$ pure, with $< 0.005\%$ water and $< 0.0005\%$ evaporation residue) were used without further purification [20].

Structural glass was obtained by fast (50 K/min) cooling each alcohol from room temperature via T_g to the boiling temperature of liquid nitrogen. T_g was 100–120 K (methanol with water impurity) [21,22], 97 K (ethanol) [1,23–27]; 98 K (1-propanol) [4,28]; 111 K (1-butanol) [20].

The thermal conductivity of the glasses of methanol, ethanol (protonated and deuterated), 1-propanol and 1-butanol was measured in a special setup [29] in the interval from 2 K to T_g using the method of flat steady-state linear flow under the equilibrium vapor pressure.

2.2. Thermal conductivity of glasses of a series of primary alcohols from methanol to 1-butanol

The thermal conductivities of glasses of primary alcohols (methanol [17], protonated [30] and deuterated [18] ethanols, 1-propanol [19] and 1-butanol [20]) are shown in Fig. 1. Note that the thermal conductivities of glasses have much lower magnitudes in comparison with corresponding equilibrium crystals in orientationally ordered phases. The temperature dependences of the thermal conductivities of the glassy alcohols follow the shapes typical of most glasses. In the low-temperature region the thermal conductivity increases with temperature, has a smeared "plateau" at $T \approx 5$–15 K, and continues to grow up to saturation at
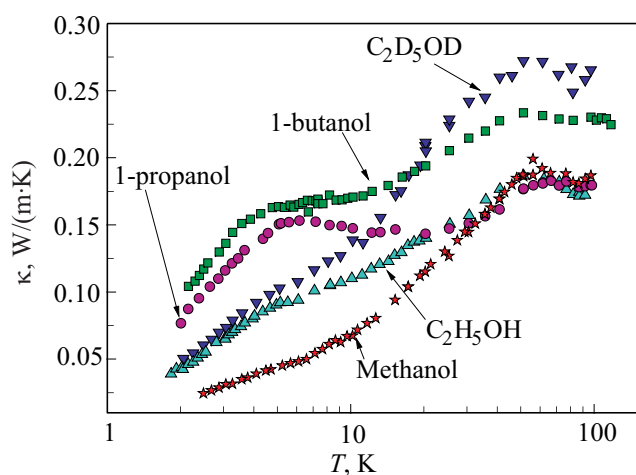
Fig. 1. The thermal conductivity of the glass state of primary alcohols — methanol [17], protonated [30] and deuterated [18] ethanol, 1-propanol [19] and 1-butanol [20] — as a function of temperature.

$T \approx 40$–50 K. 1-propanol differs from the other primary alcohols by having an extended plateau and some deflection of the thermal conductivity at $T \approx 20$ K. In the low-temperature region where heat is transferred by ballistic phonons, the thermal conductivity is observed to depend on the mass of the alcohol molecule. At low temperatures the thermal conductivity is the lowest in methanol and the highest in 1-butanol.

Figure 2 shows the thermal conductivity of primary alcohols as a function of the molecular mass at $T = 2.5$ K and 6 K. It is seen that in this region the thermal conductivity is directly proportional to the molecular mass of a simple monohydroxyl alcohol. This is a new effect. This sort of effect was first observed in primary alcohol glasses in [31] where the authors revealed that the magnitude of the thermal conductivity varied with the number of C atoms in the alcohol molecule. The measurements on the glass of deute-
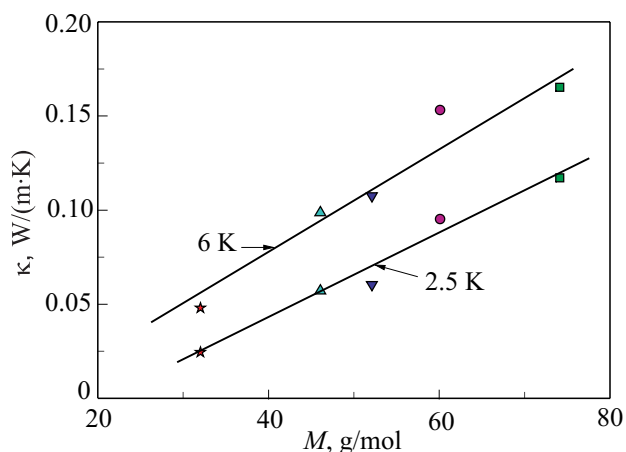

Fig. 2. The dependence of the thermal conductivity of simple alcohols upon the mass of the alcohol molecule at $T = 2.5$ K and 6 K. Symbols are experimental data, lines are linear dependences. The nomenclature is like in Fig. 1.

rated ethanol [18] prompted a more accurate conclusion that in the low-temperature region the thermal conductivity is dependent on the mass of an alcohol molecule. Such dependence is absent in the high-temperature region.

In the investigated interval of temperatures the temperature dependence of the thermal conductivity of alcohol glasses can be presented as a sum of two contributions:

$$\kappa(T) = \kappa_I(T) + \kappa_{II}(T),$$

where $\kappa_I(T)$ is the contribution of ballistic acoustic phonons (phenomenological soft potential model [13,17,31]) and $\kappa_{II}(T)$ is the contribution of local phonon modes (phenomenological Caholl–Pohl model [32–34]). The contribution $\kappa_{II}(T)$ becomes dominant in the temperature region of high Bose-peak energies.

2.3. Thermal conductivity of orientational glass of ethanol

Of all the investigated alcohols, only ethanol (protonated and deuterated) can be obtained in the state of orientational glass. The orientational glass is a bcc structure with the centers of masses at the lattice sites which has no orientational order of molecules. The orientational glass of protonated [30] and deuterated [18] ethanol was obtained by cooling a plastic crystal (RPC). A liquid room temperature was cooled at a quite high rate of ≈ 1.5 K/min to avoid crystallization of the orienationally ordered phase and to obtain a plastic crystal. The plastic crystal, which is a crystalline bcc phase with a dynamic orientational disorder, appeared at $T \approx 125$ K. The cooling was continued at the same rate, and an orientational glass of ethanol was obtained when the plastic crystal was passing through the temperature of the transition to an orientationally disordered phase. This temperature coincides with T_g in protonated and deuterated ethanols. The moments of the liquid–plastic crystal and plastic crystal–orientational glass phase transitions show up as kinks in the curves in the thermogram of sample preparation.

The thermal conductivities of protonated and deuterated ethanols in two states (SG and OG) [18] are illustrated in Fig. 3. It is seen that the temperature behavior of the thermal conductivities of theses glasses is closely similar. Their magnitudes practically coincide at low temperatures. As the temperature rises, the thermal conductivity of glasses at first increases fast, then the growth rate becomes significantly slower at $T \approx 5$–15 K and finally the thermal conductivity reaches saturation at $T \approx 51$ K. The difference between the glasses is that the thermal conductivity of the deuterated ethanol SG and OG grows faster with temperature and its thermal conductivity in saturation are about 1.4 times higher than in the case of protonated alcohol. Besides, it is seen that the difference between the thermal conductivities of orientational and structural glasses of the deuterated ethanol is less than the difference between the corresponding glasses of protonated ethanol.
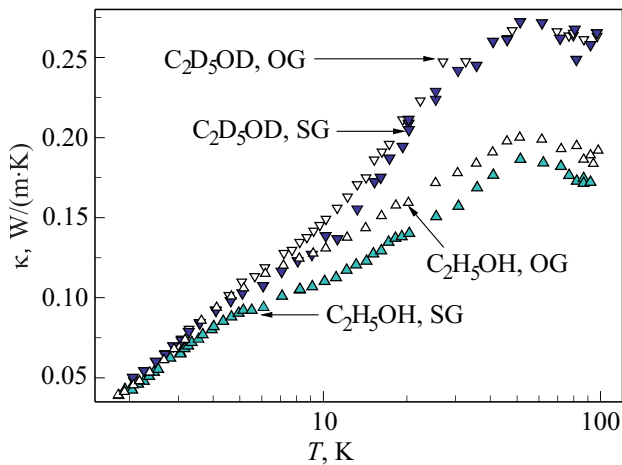
Fig. 3. The temperature dependences of the thermal conductivity of protonated and deuterated ethanol in the SG and OG states [18].

The thermal conductivity $\kappa(T)$ of the SG and OG of protonated and deuterated ethanols can be presented as a sum of two contributions $\kappa_I(T)$ and $\kappa_{II}(T)$ in the whole interval of the investigated temperatures. $\kappa_I(T)$ describes the contribution of propagating phonons which are the main heat carries (soft potential model [13,18]). $\kappa_{II}(T)$ is due to short-wavelength localized vibrational modes, or phonons whose mean free path is half the wavelength of a phonon (phenomenological Cahill–Pohl model [32–34]). The effect of complete deuteration in SG and OG manifests itself in the temperature behavior of the contribution $\kappa_{II}(T)$ which grows with temperature faster than in the protonated ethanol.

It is interesting that the thermal conductivities of OG and SG of deuterated and protonated ethanols are very close though these glasses have basically different molecular disorders. The behavior of the thermal conductivities of OG of protonated and deuterated ethanols differs drastically from that in completely ordered crystals [18]. Besides, the thermal conductivities of OGs of protonated and deuterated ethanol are much lower than the thermal conductivity of the corresponding equilibrium crystals in orientationally ordered phases.

2.4. Structural transformations in ethanol

As mentioned above, among the simple alcohols, ethanol is noted for its rich polymorphism. Each of its states — structural glass, orientational glass, a fully orientationally ordered crystal — has distinctive features that are clearly evident in the temperature behavior of the thermal conductivity. The effect of thermal conductivity relaxation caused by annealing the sample was first observed on ethanol in the fully-ordered phase formed due to the OG→RPC→FOC transition. This result is new and rather unexpected. Note that additional experiments on a solid deuterated ethyl alcohol supported the absence of this effect in it. In four samples of deuterated ethyl

alcohol the heating of the RPC phase provoked violent spontaneous crystallization to the orientationally ordered phase at different temperatures: near $T = 115$, 119, 127 and 148 K. The values of $\kappa(T)$ of the four samples in the orientationally ordered crystalline phase coincided within the experimental error and corresponded to the thermal conductivity of the well-annealed FOC sample [18].

The RPC→FOC transition of protonated ethyl alcohol was carried out at the average temperature $T = 109$ K. In the course of the transition the thermal conductivity increased slowly and exponentially with time $\kappa(t) = \kappa(\infty) - \Delta\kappa \exp(-t/\tau)$ ($\tau = 58.5$ h is the characteristic relaxation time, $\Delta\kappa = 0.095$ W/(m·K) is the change in the thermal conductivity) for 200 h (see Fig. 4). When $\kappa(t)$ stopped growing and reached its saturation $\kappa(\infty) = 0.214$ W/(m·K), the thermal conductivity $\kappa(T)$ was measured as a function of temperature in the interval $T = 109$–2 K. The dependence $\kappa(T)$ corresponding to the structure α_1 of FOC (see Fig. 5, curve α_1) was noticeably different from $\kappa(T)$ of an orientational glass.

Further relaxation of the thermal conductivity $\kappa(t)$ was observed for 70 h at $T = 124$ K with the characteristic relaxation time $\tau = 24$ h and $\Delta\kappa = 0.013$ W/(m·K) (see Fig. 4). The dependence $\kappa(T)$ taken after the relaxation at $T = 124$ K is shown in Fig. 5 (curve α_2). This dependence corresponds to the new relaxed monoclinic structure α_2 of FOC whose thermal conductivity is considerably higher than that of FOC α_1.

The annealing of the FOC α_2 structure in the premelting region at 156 K, where the monoclinic structure FOC-β is formed, led to a fast sharp increase in $\kappa(T)$ of FOC-β (Fig. 5). The dependences $\kappa(t)$ taken at different temperatures (109, 124 and 156 K) are shown in Fig. 4.
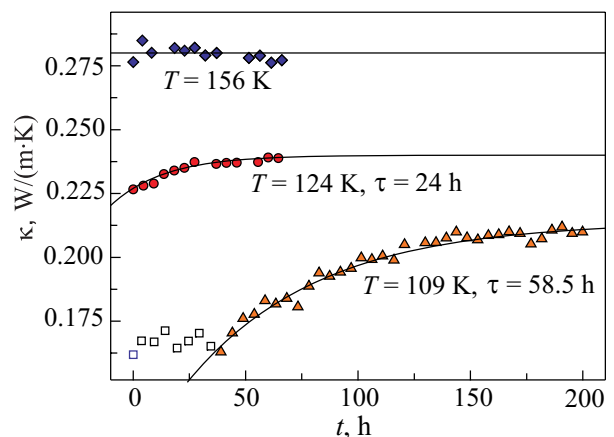

Fig. 4. Thermal conductivity relaxation during SG→SCL→RPC (□), and RPC→FOC phase transitions at $T = 109$ K (▲); subsequent annealing of FOC at the average $T = 124$ K (•) and $T = 156$ K (♦). Lines are calculated dependences $\kappa(t) = \kappa(\infty) - \Delta\kappa \exp(-t/\tau)$, where τ is the characteristic relaxation time, $\Delta\kappa$ is the change in the thermal conductivity, $\kappa(\infty)$ is the thermal conductivity of saturation.
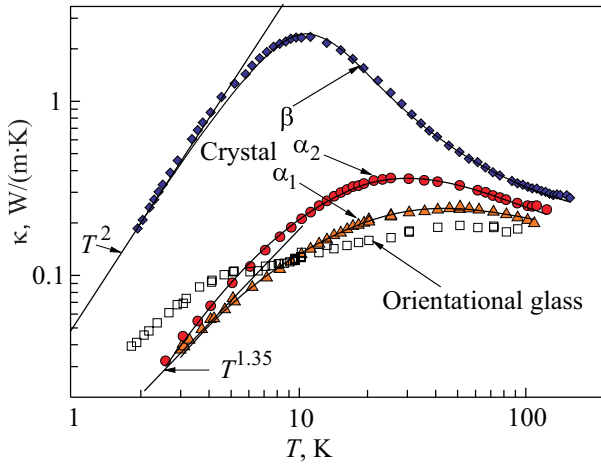
Fig. 5. The temperature dependences of the thermal conductivity of solid ethanol sample in various structural states: OG (□) [30], after annealing FOC at $T = 109$ K (structure α_1 (▲)), 124 K (structure α_2 (•)) and 156 K (structure β (♦)). Lines — fitting the experimental data with the theoretical curves calculated within the Debye–Peierls model [8]. Straight lines — the dependences $\kappa(T) \sim T^2$ and $\kappa(T) \sim T^{1.35}$.

The dependences $\kappa(T)$ for different FOC structures are illustrated in Fig. 5. It is seen (see Fig. 5) how the curve $\kappa(T)$ of OG phase transforms into the curve $\kappa(t)$ of the thermodynamically equilibrium phase of a FOC with low contents of defects (structure β) passing in turn through various structural states (monoclinic structures α_1 and α_2) at increasing of annealing temperature. The curves describing the thermal conductivity of completely orientationally ordered crystals FOC ($\alpha_1, \alpha_2, \beta$) are similar to the curves $\kappa(T)$ with a phonon maximum that are typical for dielectric crystals. The sample obtained through the solid phase transformation at $T = 109$ K (structure α_1) has an anomalously low thermal conductivity. At low temperatures the thermal conductivity is considerably lower than $\kappa(T)$ of the OG crystal. $\kappa(T)$ grows with increasing temperature and at $T \approx 8$ K becomes equal to the thermal conductivity of the OG crystal. The fact that at low temperatures the thermal conductivity of the FOC crystal with the structure α_1 is even lower than the thermal conductivity of OG suggests that the α_1 phase of FOC is most likely an intermediate state with a large number of defects. Below 8 K the thermal conductivity of crystal with structure α_1 is proportional to $T^{1.35}$, which suggests intensive phonon scattering by point and linear defects. As the temperature rises, the thermal conductivity increases and reaches its maximum $\kappa_{max} \approx 0.25$ W/(m·K), which is only 20% higher than κ_{max} of the OG crystal. The smeared maximum in the thermal conductivity of crystal with structure α_1 appears at a temperature identical with that of the κ_{max} of the OG crystal ($T = 51$ K).

After annealing at $T = 124$ K, the crystal with structure α_1 transforms into a crystal with structure α_2. Its maxi-

mum thermal conductivity ($\kappa_{max} \approx 0.36$ W/(m·K)) exceeds κ_{max} of the structure α_1 and the temperature of the maximum shifts toward low-temperatures ($T_{max} = 25.3$ K). The κ-curves of α_2 and OG structures intersect at $T \approx 5.5$ K; below this temperature the thermal conductivity of the crystal with structure α_2 is lower than $\kappa(T)$ of the OG but higher than $\kappa(T)$ of the crystal with structure α_1. In the low-temperature region the thermal conductivity of crystal with structure α_2 rises more steeply than in the crystal with structure α_1 and is proportional to $T^{1.7}$. This indicates that the structure α_2 is superior to the structure α_1 in quality and has fewer defects. The crystal with structure β obtained by annealing the crystal with structure α_2 at $T \approx 156$ K has the highest thermal conductivity which is about an order of magnitude higher than $\kappa(T)$ of the crystal with structure α_1 at low temperatures. In this series the crystal with structure β is noted for the highest quality and the lowest contents of defects. It has a distinct maximum of thermal conductivity ($\kappa_{max} = 2.32$ W/(m·K)) which is almost an order of magnitude higher than κ_{max} of the crystal with structure α_1. It occurs at $T_{max} = 11.2$ K. Below T_{max} the thermal conductivity of the crystal with structure β is proportional to the quadratic temperature dependence, which corresponds to the scattering of phonons by linear defects (dislocations).

Figure 5 shows the temperature dependences $\kappa(T) \sim T^2$ and $\kappa(T) \sim T^{1.35}$ (straight lines) along with the fitting of the experimental results for FOC ($\alpha_1, \alpha_2, \beta$) to the theoretical curves calculated within the Debye–Peierls model [8] allowing for the resistive U-processes of phonon scattering and the phonon scattering by point and linear defects. It is seen that the model describes quite accurately the experiment data for the three completely orientationally ordered crystals. The difference in the thermal conductivities of the FOC-α_1 structure and FOC-β structure may be connected with improving quality of the crystals in the course of annealing. The theoretical curves and the experimental data on $\kappa(T)$ were fitted using the procedure of [35] and taking into account the U-processes of scattering and the phonon scattering at point and linear defects. The best fitting parameters are given in Table 1. Note that the annealing of the sample with increasing annealing temperature weakens mainly the phonon scattering at point and linear defects.

Table 1. The parameters obtained from fitting theoretical curves to experimental data. The relaxation rates of resistive U-processes of scattering are: $\tau_U^{-1}(\omega, T) = B\omega^2 T \exp(-E_U / T)$, $B = 3.88 \cdot 10^{-16}$ s / K, $E_U = 27$ K; scattering at dislocations $\tau_{dis}^{-1}(\omega) = D_{dis}\omega$ and at point defects $\tau_R^{-1}(\omega) = C\omega^4$. The Debye temperature is $\Theta_D = 112$ K, the sound velocity is $v = 1600$ m/s [35]

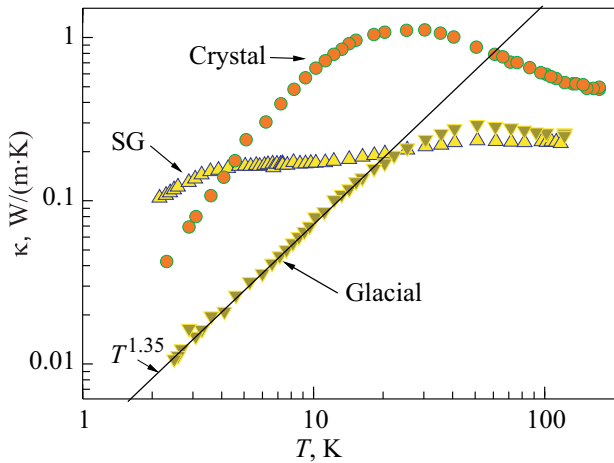| Sample, structure	D_{dis}	C, s^3
α_1	$1.22 \cdot 10^{-2}$	$6.75 \cdot 10^{-40}$
α_2	$1.22 \cdot 10^{-2}$	$1.69 \cdot 10^{-40}$
β	$1.07 \cdot 10^{-3}$	$2.15 \cdot 10^{-42}$

Fig. 6. The temperature dependences of the thermal conductivity of 1-butanol in three states: SG (Δ), "glacial" (∇) and stable crystal ($\circ$). Data of [20] and [36]. Straight line is the dependence $\kappa(T) \sim T^{1.35}$.

This shows up in the behavior of the parameters: the parameter characterizing the phonon scattering at linear defects jumps down as the structure changes from α to β; the parameter describing the phonon scattering at point defects decreases monotonically as the structure transforms from α_1 via α_2 to β.

It is interesting that the κ values in the curve of the structure α_1 with the highest content of defects are very low (see Fig. 5). This is a basically new result obtained for the first time on an ethanol sample. A much similar behavior of the thermal conductivity was observed previously on a sample of 1-butanol in its exotic metastable so-called "glacial" state [20,36] (see Fig. 6). The state (its nature has been discussed much in literature [37–39]) was obtained from a supercooled liquid at $T \approx 122$ K. At low temperatures the thermal conductivity of "glacial" 1-butanol is dependent on temperature as $T^{1.35}$ [36]. The highest $\kappa(T)$ of the "glacial" 1-butanol state occurs at $T = 51$ K which is T_{max} of 1-butanol structural glass (Fig. 6). Besides, κ_{max} of the "glacial" state is about 25% higher than κ_{max} of 1-butanol structural glass. The similarity of the thermal conductivities of "glacial" state of 1-butanol and ethanol obtained through the solid-state RPC-FOC phase transition (Fig. 5, curve α_1) suggests a common origin of both.

3. Conclusions

New features have been revealed in the temperature behavior of the thermal conductivity of simple alcohol in the glass state.

— It has been found that in the low-temperature region the thermal conductivity of the structural glass of the alcohols in the series from methanol to 1-butanol has linear dependence on the mass of the alcohol molecule. It is shown that the thermal conductivity of structural glass can be presented in the investigated temperature interval as a sum of two contributions $\kappa(T) = \kappa_I(T) + \kappa_{II}(T)$, where $\kappa_I(T)$ and $\kappa_{II}(T)$ are contributed by ballistic acoustic phonons (soft potential model) and local modes (Cahill–Pohl model), respectively.

— It has been revealed that deuteration of ethanol affects the thermal conductivity in both structural and orientational glasses. The effect of complete deuteration is evident in the temperature behavior of the contribution $\kappa_{II}(T)$.

— A comparison of the temperature behavior of the thermal conductivity of protonated and deuterated ethanol in states of structural and orientational glass and in phase of fully orientationally ordered crystal has shown that the molecular orientational disorder is the main source of scattering acoustic phonons.

The annealing effect was observed in the orientationally ordered phase of solid protonated ethanol which was obtained due to a solid-state transition from an orientationally disordered crystal. The investigation of the structural transformations in protonated ethanol by measuring thermal conductivity has shown that the fully orientationally ordered crystal phase obtained by heating of orientational glass and its annealing at $T = 109$ K exhibits an anomalously low thermal conductivity. The temperature behavior of the thermal conductivity of this fully orientationally ordered crystal sample is closely similar to that of 1-butanol in the so-called "glacial" state, which suggests their identical origin.

1. M.A. Ramos, S. Vieira, F.J. Bermejo, J. Dawidowski, H.E. Fisher, H. Schober, M.A. González, C.K. Loong, and D.L. Price, *Phys. Rev. Lett.* **78**, 82 (1997).
2. M.A. Ramos and U. Buchenau, *Phys. Rev.* **B55**, 5749 (1997).
3. C. Talón, M.A. Ramos, S. Vieira, G.J. Cuello, F.J. Bermejo, A. Criado, M.L. Senent, S.M. Bennington, H.E. Fischer, and H. Schober, *Phys. Rev.* **B58**, 745 (1998).
4. C. Talón, M.A. Ramos, S. Vieira, I. Shmyt'ko, N. Afanisova, A. Criado, G. Madariaga, and F.J. Bermejo, *J. Non-Cryst. Solids* **287**, 226 (2001).
5. M.A. Ramos, C. Talón, R.J. Jiménez-Riobóo, and S. Vieira, *J. Phys.: Condens. Matter* **15**, S1007 (2003).
6. M. Kveder, D. Merunka, M. Jokic, J. Makarevic, and B. Rakvin, *Phys. Rev.* **B80**, 052201 (2009).
7. D. Lamoen and N.H. March, *Phys. Lett.* **A373**, 799 (2009).
8. R. Berman, *Thermal Conduction in Solids,* Clarendon Press, Oxford (1976).
9. P.W. Anderson, B.I. Halperin, and C.M. Varma, *Philos. Mag.* **25**, 1 (1972).
10. W.A. Philips, *J. Low Temp. Phys.* **7**, 351 (1972).
11. D. Tielbürger, R. Merz, R. Ehrenfels, and S. Hunklinger, *Phys. Rev.* **B45**, 2750 (1992).
12. D.A. Parshin, *Phys. Rev.* **B49**, 9400 (1994).

13. U. Buchenau, Yu.M. Galperin, V.L. Gurevich, D.A. Parshin, M.A. Ramos, and H.R. Schober, *Phys. Rev*. **B46**, 2798 (1992).

14. O. Haida, H. Suga, and S. Seki, *J. Chem. Thermodyn*. **9**, 1133 (1977).

15. M.A. Ramos, I.M. Shmyt'ko, E.A. Arnautova, R.J. Jiménez-Riobóo, V. Rodríguez-Mora, S. Vieira, and M.J. Capitán, *J. Non-Cryst. Solids* **352**, 4769 (2006).

16. F.J. Bermejo, D. Martin, J.L. Martínez, F. Batallan, M. García-Hernández, and F.J. Mompean, *Phys. Lett*. **A150**, 201 (1990).

17. O.A. Korolyuk, A.I. Krivchikov, I.V. Sharapova, and O.O. Romantsova, *Fiz. Nizk. Temp*. **32**, 380 (2009) [*Low Temp. Phys*. **32**, 290 (2009)].

18. A.I. Krivchikov, F.J. Bermejo, I.V. Sharapova, O.A. Korolyuk, and O.O. Romantsova, *Fiz. Nizk. Temp*. **37**, 651 (2011) [*Low Temp. Phys*. **37**, 517 (2011)].

19. A.I. Krivchikov, A.N. Yushchenko, O.A. Korolyuk, F.J. Bermejo, R. Fernandez-Perea, I. Bustinduy, and M.A. González, *Phys. Rev*. **B77**, 024202 (2008).

20. M. Hassaine, R.J. Jiménez-Riobóo, I.V. Sharapova, O.A. Korolyuk, A.I. Krivchikov, and M.A. Ramos, *J. Chem. Phys*. **131**, 174508 (2009).

21. F.J. Bermejo, M. García-Hernández, J.L. Martínez, A. Criado, and W.S. Howells, *J. Chem. Phys*. **96**, 7696 (1992).

22. F.J. Bermejo, J. Alonso, A. Criado, F.J. Mompean, J.L. Martinez, M. Garcia-Hernandez, and A. Chahid, *Phys. Rev*. **B46**, 6173 (1992).

23. A. Criado, M. Jiménez-Ruiz, C. Cabrillo, F.J. Bermejo, M. Grimsditch, H.E. Fischer, S.M. Bennington, and R.S. Eccleston, *Phys. Rev*. **B61**, 8778 (2000).

24. M. Jiménez-Ruiz, A. Criado, F.J. Bermejo, G.J. Cuello, F.R. Trouw, R. Fernández-Perea, H. Löwen, C. Cabrillo, and H.E. Fischer, *Phys. Rev. Lett*. **83**, 2757 (1999).

25. C. Cabrillo, F.J. Bermejo, M. Jiménez-Ruiz, M.T. Fernández-Díaz, M.A. González, and D. Martín y Marero, *Phys. Rev*. **B64**, 064206 (2001).

26. H.E. Fischer, F.J. Bermejo, G.J. Cuello, M.T. Fernández-Díaz, J. Dawidowski, M.A. González, H. Schober, and M. Jimenez-Ruiz, *Phys. Rev. Lett*. **82**, 1193 (1999).

27. M.A. Miller, M. Jiménez-Ruiz, F.J. Bermejo, and N.O. Birge, *Phys. Rev*. **B57**, R13977 (1998).

28. R.C. Whilhoit and B.J. Zwolinski, *J. Phys. Chem. Ref. Data* **2**, Suppl. 1, 1 (1973).

29. A.I. Krivchikov, B.Ya. Gorodilov, and O.A. Korolyuk, *Instrum. Exp. Tech*. **48**, 417 (2005).

30. A.I. Krivchikov, A.N. Yushchenko, V.G. Manzhelii, O.A. Korolyuk, F.J. Bermejo, R. Fernandez-Perea, C. Cabrillo, and M.A. González, *Phys. Rev*. **B74**, 060201® (2006); F.J. Bermejo, R. Fernandez-Perea, C. Cabrillo, A.I. Krivchikov, A.N. Yushchenko, O.A. Korolyuk, V.G. Manzhelii, M.A. Gonzalez, and M. Jimenez-Ruiz, *Fiz. Nizk. Temp*. **33**, 790 (2007) [*Low Temp. Phys*. **33**, 606 (2007)].

31. A.I. Krivchikov, O.A. Korolyuk, I.V. Sharapova, O.O. Romantsova, F.J. Bermejo, C. Cabrillo, R. Fernandez-Perea, and I. Bustinduy, *J. Non-Cryst. Solids* **357**, 483 (2011).

32. D.G. Cahill and R.O. Pohl, *Phys. Rev*. **B35**, 4067 (1987).

33. D.G. Cahill, S.K. Watson, and R.O. Pohl, *Phys. Rev*. **B46**, 6131 (1992).

34. V.A. Konstantinov, V.G. Manzhelii, V.P. Revyakin, and V.V. Sagan, *Fiz. Nizk. Temp*. **31**, 553 (2005) [*Low Temp. Phys*. **31**, 419 (2005)]; V.A. Konstantinov, V.G. Manzhelii, V.P. Revyakin, and V.V. Sagan, *Fiz. Nizk. Temp*. **32**, 1414 (2006) [*Low Temp. Phys*. **32**, 1076 (2006)].

35. A.I. Krivchikov, F.J. Bermejo, I.V. Sharapova, O.A. Korolyuk, and O.O. Romantsova, *Fiz. Nizk. Temp*. **35**, 1143 (2009) [*Low Temp. Phys*. **35**, 891 (2009)].

36. A.I. Krivchikov, M. Hassaine, I.V. Sharapova, O.A. Korolyuk, R.J. Jiménez-Riobóo, and M.A. Ramos, *J. Non-Cryst. Solids* **357**, 524 (2011).

37. B.V. Bol'shakov and A.G. Dzhonson, *Dokl. Phys. Chem*. **393**, 318 (2003).

38. B.V. Bol'shakov and A.G. Dzhonson, *J. Non-Cryst. Solids* **351**, 444 (2005).

39. I.M. Shmyt'ko, R.J. Jiménez-Riobóo, M. Hassaine, and M.A. Ramos, *J. Phys.*: *Condens. Matter* **22**, 195102 (2010).